ORIGINAL ARTICLE

On the seismic collapse capacity of optimally designed steel braced frames

Saeed Gholizadeh[1] · Aydin Hassanzadeh[1] · Arman Milany[1] · Hamid Farrokh Ghatte[2]

Abstract

The main purpose of this study is to respond to an important question in the field of structural engineering: is the seismic collapse capacity of optimally designed concentrically steel braced frames acceptable or not? The present work includes two phases: performance-based design optimization and seismic collapse safety assessment. In the first phase, three nature-inspired metaheuristic algorithms, namely improved fireworks algorithm, center of mass optimization, and enhanced colliding-bodies optimization are employed to carry out the optimization task. In the second phase, seismic collapse capacity of the optimally designed concentrically steel braced frames is evaluated by performing incremental dynamic analysis and generating fragility curves. Two design examples of 5- and 10-story concentrically steel braced frames with two different topologies of braces are presented. The numerical results indicate that the center of mass optimization algorithm outperforms the other algorithms. However, all of the optimal designs found by all algorithms are of acceptable seismic collapse safety.

Keywords Performance-based design · Optimization · Incremental dynamic analysis · Seismic safety · Fragility assessment · Concentrically braced frame

1 Introduction

The implementation of classic performance-based design (PBD) is based on the selection of a set of performance objectives defined in terms of performance levels and seismic hazards [1]. In the framework of PBD, structural responses evaluated with the aid of nonlinear structural analysis need to be compared with acceptable limits which are known as acceptance criteria. These limits are categorized into two groups, inter-story drift (global level) and component demand limits (local level). In recent years, PBD methodologies have been incorporated in the structural optimization processes, and a few studies have been conducted in this area. Fragiadakis et al. [2] have done an overview of procedures for seismic assessment of structures. They have mentioned that to decrease the seismic risks, engineers should estimate the seismic safety of structures. Gholizadeh

and Fattahi [3] have proposed a multi-objective metaheuristic algorithm to optimize steel frames considering seismic collapse safety of the frames. Hassanzadeh and Gholizadeh [4] proposed a methodology to determine the optimal placement of the braces in concentrically steel braced frames (CBFs) in the framework of PBD. Degertekin et al. [5] proposed a school-based optimization algorithm for the design of steel frames in the context of PBD.

One of the major concerns in the field of structural engineering is to assess the seismic safety of the structures and one of the best ways to achieve this is the implementation of incremental dynamic analysis (IDA). The basic principles of IDA were presented by Bertero [6]. It was then introduced to the seismic hazard analysis of nonlinear systems, mainly for drift demand evaluation of frame structures [7]. Cornell and Vamvatsikos [8, 9] presented the principles for the IDA procedure and verified its efficiency on steel moment frames. Brunesi et al. [10] investigated the progressive collapse assessment of low-rise reinforced concrete frames by implementing fragility analysis.

CBFs are commonly used lateral-load resisting structural systems in seismic prone regions. During the last decades, extensive studies have been achieved on the different aspects of these structures [11, 12]. In recent years, metaheuristic

✉ Saeed Gholizadeh
  s.gholizadeh@urmia.ac.ir

[1] Department of Civil Engineering, Urmia University, Urmia, Iran

[2] Civil Engineering Department, Faculty of Engineering, Antalya Bilim University, Antalya, Turkey

algorithms, which are more applicable and efficient than gradient-based methods, have been utilized to tackle sophisticated structural optimization problems. The present study deals with the PBD optimization of CBF structures using three physics-based metaheuristic algorithms. For this purpose, improved fireworks algorithm (IFWA) [13], center of mass optimization (CMO) [14], and enhanced colliding-bodies optimization (ECBO) [15] are employed in the present work. To assess the seismic collapse safety of optimally designed CBFs, fragility curves are generated by performing IDA based on the methodology of FEMA-P695 [16]. Two design examples including 5- and 10-story concentrically steel braced frames with two different patterns of placement of braces in the frames are illustrated. The obtained results demonstrate that all the performance-based optimally designed CBFs have acceptable seismic collapse capacity.

2 Formulation of PBD optimization problem

Performance objectives of the present study are as follows: immediate occupancy (IO), life safety (LS) and collapse prevention (CP) performance levels correspond, respectively, to 50%, 10%, and 2% probability of exceedance in 50 years. Moreover, pushover analysis, based on the displacement coefficient method [1], is implemented to evaluate the seismic structural response of CBFs, in which target displacement is defined as follows:

$$\delta_t = C_0 C_1 C_2 S_a \frac{T_e^2}{4\pi^2} g, \tag{1}$$

where δ_t is the target displacement, C_0 is a modification factor linking spectral displacement for an equivalent SDOF system to the roof displacement of a multistory structure, and C_1 and C_2 are modification factors to consider the effects of inelastic system degradation and $P-\Delta$ effects, respectively [1]. Furthermore, T_e represents the effective fundamental period, g is gravity acceleration, and S_a is spectral acceleration.

In this study, OpenSees Platform [17] is utilized to perform pushover and incremental dynamic analyses and other required computer programs in the optimization process are coded in MATLAB [18].

Design variables For the PBD optimization problem of CBFs, the vector of design variables, X, is defined as follows:

$$X = \{x_{C1} \ldots x_{Ci} \ldots x_{Cnc} \, x_{B1} \ldots x_{Bj} \ldots x_{Bnb} \, x_{BR1} \ldots x_{BRk} \ldots x_{BRnbr}\}^T \tag{2}$$

where x_{Ci}, x_{Bj}, and x_{BRk} are sizing design variables of ith group of columns, jth group of beams and kth group of

braces, respectively; nc, nb and nbr, respectively, denote the number of columns, the number of beams and the number of braces included in the structure.

Design constraints Geometric, strength, and PBD constraints are considered during the optimization process of CBFs. The geometric constraints are checked to ensure the consistency of dimensions of beams and columns in all framing joints [14]. As per the strength constraints, all structural elements must be checked for the gravity load combinations based on LRFD-AISC [19]. To check the PBD constraints, pushover analysis is conducted to evaluate the structural response at each performance level. The inter-story drift constraint (g_{ISD}) for each hazard level can be defined as follows:

$$g_{ISD} = \frac{ISD}{ISD_{all}} - 1, \tag{3}$$

where ISD is the maximum inter-story drift at each performance level and ISD_{all} is its acceptance limit.

The plastic rotation constraint (g_{PR}) for the deformation-controlled columns at each performance level is formulated as follows:

$$g_{PR} = \frac{\theta}{\theta_{all}} - 1 \tag{4}$$

where θ and θ_{all} are, respectively, maximum plastic rotation and permissible plastic rotation demands at each performance level according to ASCE 41-13 [1].

The following constraint for the force-controlled columns (g_{FC}) should be satisfied:

$$g_{FC} = \frac{P_{UF}}{P_{cl}} + \frac{M_{UF}}{M_{cl}} - 1, \tag{5}$$

where P_{UF} and M_{UF} are axial force and moment of column due to the combination of gravity and seismic loads at each performance level, respectively. P_{cl} and M_{cl} are, respectively, lower-bound compression and moment strength of the column.

The axial deformation constraint (g_{AD}) of the braces at each performance level is expressed as follows:

$$g_{AD} = \frac{\Delta}{\Delta_{all}} - 1 \tag{6}$$

where Δ and Δ_{all} are, respectively, the absolute axial deformation of the braces and its permissible values at each performance level according to ASCE 41-13 [1].

Equation (6) is additionally employed to control the axial deformation of the columns in tension.

Objective function The main purpose of this study is to minimize the structural weight of the CBFs, and the objective function is formulated as:

$$W(X) = \sum_{i=1}^{ne} \rho_i \times V_i, \tag{7}$$

where W is structural weight; ρ_i and V_i are the weight density and volume of ith element, respectively; and ne is the number of elements.

To implement the design constraints in the optimization process, the exterior penalty function method (EPFM) [20] is utilized. In this case, the pseudo-objective function, Φ, is represented as follows:

$$\Phi(X, r_p) = W(X) \times \left(1 + r_p \sum_{m=1}^{ng} \left(\max \left\{ 0, g_m(X) \right\} \right)^2 \right), \tag{8}$$

where r_p and ng are a penalty coefficient and the number of design constraints, respectively.

3 Metaheuristic algorithms

In this work, three different metaheuristic algorithms, improved fireworks algorithm, center of mass optimization, and enhanced colliding-bodies optimization are used as the optimizers. The basic concepts of these metaheuristic algorithms are explained below.

3.1 Improved fireworks algorithm

Fireworks algorithm (FWA) is based on the simulation of fireworks explosion to a kind of search process [21]. The sky, including fireworks, refers to a response domain, and the sparks explosion represents evaluation and searches for answers. The updating process, the selection and generation of next stage fireworks, are repeated until the best solution is found. Various studies have been conducted to improve this algorithm [22] and one of them is an improved fireworks algorithm (IFWA) summarized as follows:

i. A total number of n fireworks are randomly initialized and their objective values are calculated. The best positions are selected as the next stage firework.

ii. The explosion amplitude, A_0, and the number of sparks are specified. The best number of sparks is determined by sensitivity analysis and the amplitude is taken as a function of lower and upper bounds of design variables (i.e., X_L and X_U) as follows:

$$A_0 = 0.5(X_L + X_U) \tag{9}$$

iii. The spark generation is achieved as follows:

$$\hat{X}(t+1) = X(t+1) + R_1(t) \cdot A(t) + R_2(t) \cdot (X(t+1) - X(t)) \tag{10}$$

where R_1 and R_2 are random value vectors in $[-1, +1]$ interval; $X(t)$ is a firework in iteration t.

iv. If the best spark in current iteration ($\hat{X}^{\text{fittest}}(t)$) is better than the corresponding firework, $X(t)$, it will be selected as the next step firework, and its amplitude will be expanded by an amplification factor (C_A):

$$A(t+1) = C_A \cdot A(t) \tag{11}$$

Otherwise, it will not be updated and the explosion amplitude will contract by a reduction coefficient (CR) to narrow down the search domain:

$$A(t+1) = C_R \cdot A(t) \tag{12}$$

The values of C_A and C_R are of the most important components in IFWA, which should be determined by sensitivity analysis.

v. The search for optimum solution process is carried out until a termination criterion is satisfied.

3.2 Center of mass optimization

Center of mass optimization (CMO) algorithm is inspired by the theory of the center of mass. As the mass of search agents are smaller, their distance to the center of mass will be larger and vice versa. The mass of ith particle, X_i, is determined as follows:

$$m_i = \frac{1}{\Phi(X_i, r_p)} . \tag{13}$$

In each iteration, particles are sorted and divided into two groups based on their masses. The sorted particles in the first group are paired with their corresponding ones in the second group. The ability to establish a suitable balance between exploration and exploitation is one of the essential characteristics of the CMO algorithm. The particles' position updating in the CMO algorithm is as follows:

i. A controlling parameter (CP) whose value is decreased from 1.0 in the first iteration to 0.0 in the last iteration ($t_{\max}$) is defined as follows:

$$CP(t) = \exp(-5t/t_{\max}) \tag{14}$$

ii. For each pair of particles, in iteration t, the position of center of mass (X^C) and the distance (D) of the particles are evaluated as follows:

$$X^C(t) = \frac{m_{g1} X_{g1}(t) + m_{g2} X_{g2}(t)}{m_{g1} + m_{g2}} \tag{15}$$

$$D(t) = \left| X_{g1}(t) - X_{g2}(t) \right| \tag{16}$$

where X_{g1} and X_{g2} are particles in the first and second groups, respectively, and m_{g1} and m_{g2} are their corresponding masses.

iii. In exploration stage, the updating of the position of each pair of particles is accomplished as follows:

$$\text{If } Dt > \ CP = \begin{cases} X_{g1}(t+1) = X_{g1}(t) - R_1(t).\left(X^C(t) - X_{g1}(t)\right) + R_2(t).\left(X_{best}(t) - X_{g1}(t)\right) \\ X_{g2}(t+1) = X_{g2}(t) + R_3(t).\left(X^C(t) - X_{g2}(t)\right) + R_4(t).\left(X_{best}(t) - X_{g2}(t)\right) \end{cases} \tag{17}$$

where R_1 to R_4 are the vectors of random numbers within the range of [0, 1]; X_{best} is the best solution.

iv. In exploitation stage, the position of each pair of particles is updated as follows:

$$\text{If } Dt \le \ CP = \begin{cases} X_{g1}(t+1) = X_{g1}(t) + R_5(t).\left(X_{g1}(t) - X_{g2}(t)\right) \\ X_{g2}(t+1) = X_{g2}(t) + R_6(t).\left(X_{g1}(t) - X_{g2}(t)\right) \end{cases} \tag{18}$$

where R_5 and R_6 are the vectors of random numbers generated in the range [0, 1].

3.3 Enhanced colliding-bodies optimization

The most important feature of enhanced colliding-bodies optimization (ECBO) is that this metaheuristic algorithm has no internal parameter to be tuned. The ECBO uses a mutation operator to reduce the risk of getting stuck in local optima. Moreover, it has a memory to remember some of the historically best solutions during the search process. The mass of each particle is defined by Eq. (13) and the sorted particles based on their masses are divided into stationary (S) and moving (M) groups. The particles in the group S are paired with those in the group M.

The main steps of the ECBO algorithm are as follows:

i. The velocities of particles S and M groups are evaluated according to the following formula:

$$V_S(t+1) = \left(\frac{(1+\varepsilon)m_M}{m_S + m_M}\right) V_M(t) \tag{19}$$

$$V_M(t+1) = \left(\frac{(m_M + \varepsilon m_S)}{m_S + m_M}\right) V_M(t) \tag{20}$$

$$\varepsilon = 1 - \frac{t}{t_{\max}} \tag{21}$$

ii. The updating of position of bodies in both S and M groups is implemented using the following formula:

$$X_S(t+1) = X_S(t) + R_S(t).V_S(t+1) \tag{22}$$

$$X_M(t+1) = X_M(t) + R_M(t).V_M(t+1) \tag{23}$$

where R_S and R_M are vectors of random numbers selected from the range of [−1, 1].

iii. To improve the behavior of algorithm, a parameter is introduced to decide whether to change a component of intended CB or not. The parameter pro, which is a constant value between 0 and 1 is compared with a random number rni which is taken from interval (0,1), and if rni < pro, a random component of the ith CB is selected to regenerate.

iv. To save some previously found CBs positions and their corresponding masses, a colliding memory (CM) is defined. The content of CM is updated continuously as the optimization proceeds.

4 Collapse safety assessment of CBFs

In this study, the seismic collapse safety of optimally designed CBFs is evaluated using the procedures outlined in FEMA-P695. Therefore, numerous response-history analyses must be performed for a number of far-field ground motions given in FEMA-P695 which are scaled to maximum considered earthquake (MCE). The 5% damped spectral acceleration is utilized as the intensity measure (IM), and the maximum inter-story drift is selected as the engineering demand parameter (EDP). After obtaining the IDA curves, the fragility curves must be extracted to be subsequently used in the collapse safety assessment procedure.

The collapse margin ratio (CMR) is defined as the ratio of median collapse probability where half of the records cause collapse to the spectral acceleration of the MCE intensity level.

$$CMR = \frac{IM_{50\%}}{IM_{MCE}}. \tag{24}$$

The adjusted collapse margin ratio (ACMR) is defined to consider the probabilistic scattering in the ground records which can seriously affect the collapse margin ratio. The ACMR can be calculated as follows:

$$ACMR = SSF \times CMR, \tag{25}$$

where SSF is the spectral shape factor and its values are given in Table 7-1 of FEMA-P695.

To take into account various sources of uncertainty, such as record-to-record (β_{RTR}), design requirements (β_{DR}), test

data (β_{DT}), and modeling (β_{MDL}), the total system collapse uncertainty, β_{TOT} is incorporated into the global collapse prediction procedure as calculated below:

$$\beta_{TOT} = \sqrt{\beta_{RTR}^2 + \beta_{DR}^2 + \beta_{DT}^2 + \beta_{MDL}^2}. \quad (26)$$

In this study, the values of β_{RTR}, β_{DR}, β_{DT}, and β_{MDL} are taken as 0.4, 0.1, 0.2, and 0.2, respectively [4].

5 Numerical results

The CBF structures are modeled following pinned-ended braces and beams. The nonlinear behavior of columns is modeled by a simple bilinear stress–strain relationship with strain hardening (0.3% of the elastic modulus). Moreover, for braces the uniaxial phenomenological model is considered in accordance with FEMA-274 [23]. In this work, the following collapse criteria are considered for incremental dynamic analysis [4]:

- The maximum inter-story drift reaches 0.05.
- For an IDA curve a local slope decreases to a value less than 0.2 of the elastic slope
- The nonlinear time-history structural analysis does not converge.

In this study, two design examples including three-bays, 5- and 10-story CBFs with two different placements of braces, in the middle span (MS), and the side spans (SS), are considered as shown in Fig. 1. For these examples, 30 independent PBD optimization runs are carried out by IFWA, ECBO and CMO metaheuristics and the results are compared in terms of convergence rate and the best, average, and standard deviation (SD) of optimized weight.

The modulus of elasticity and the yield stress are, respectively, 200 GPa and 344.74 MPa. The dead and live loads applied on beams are 2500 and 1000 kg/m, respectively. During the optimization process, the sections of beams, columns and beams are selected from the database of W-shaped steel sections listed in Table 1.

5.1 5-story CBF

Table 2 compares the optimal designs of 5-story CBF found by different metaheuristic algorithms. For all the methods, the number of particles and maximum number of iterations are 30 and 250, respectively. Convergence histories of best optimization runs for all algorithms are compared in Fig. 2.

It can be observed that CMO in both the MS and SS optimization cases outperforms IFWA and ECBO in terms of best weight, average weight and convergence rate.

The values of Δ/Δ_{all} of braces and inter-story drift profiles at different performance levels are, respectively, depicted in Figs. 3 and 4 for the best MS and SS designs found by IFWA. These results indicate that the axial deformation constraint of braces at IO performance level dominates the optimal designs for both the MS and SS models. Furthermore, the inter-story drifts and other responses are much less than their acceptable limits.

The IDA and collapse fragility curves of the optimal designs found by IFWA, CMO, and ECBO algorithms for MS and SS 5-story CBF are presented in Figs. 5, 6 and 7,
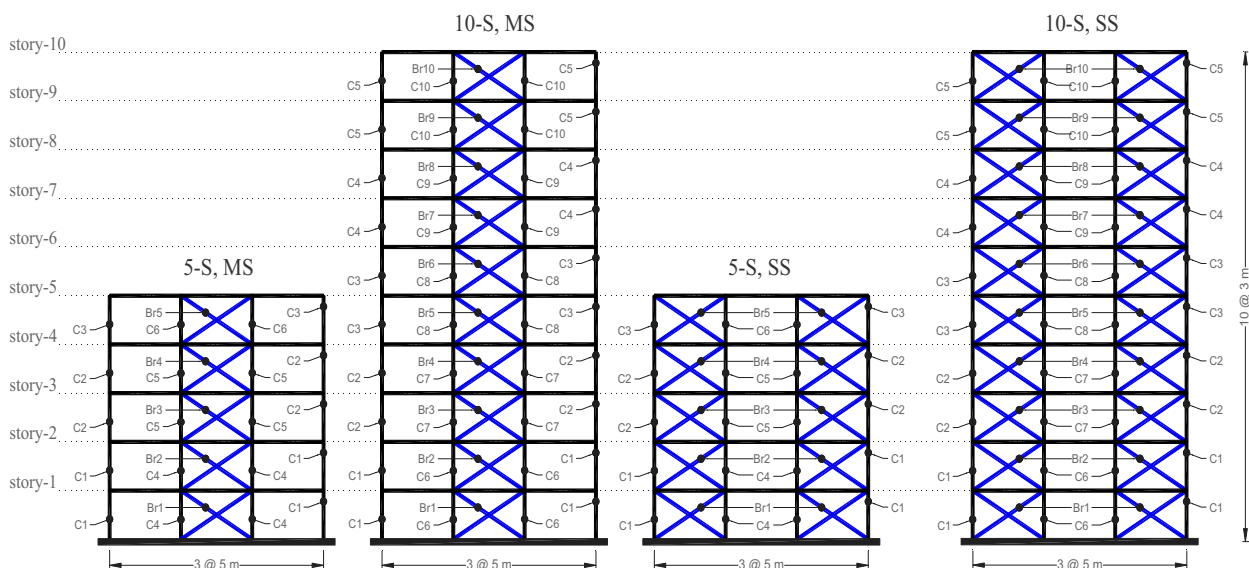

Fig. 1 Three-bays, 5- and 10-story CBFs and their grouping details

Table 1 Database of steel sections

Columns				Beams				Bracings			
No	Profile	No	Profile	No	Profile	No	Profile	No	Profile	No	Profile
1	W14×48	13	W14×257	1	W12×19	13	W21×50	1	HSS3×3×0.188	13	HSS5×5×0.500
2	W14×53	14	W14×283	2	W12×22	14	W21×57	2	HSS3×3×0.250	14	HSS6×6×0.500
3	W14×68	15	W14×311	3	W12×35	15	W24×55	3	HSS3×3×0.313	15	HSS6×6×0.625
4	W14×74	16	W14×342	4	W12×50	16	W21×68	4	HSS3×3×0.375	16	HSS8×8×0.500
5	W14×82	17	W14×370	5	W18×35	17	W24×62	5	HSS3-1/2×3–1/2×0.313	17	HSS7×7×0.625
6	W14×132	18	W14×398	6	W16×45	18	W24×76	6	HSS3-1/2×3–1/2×0.375	18	HSS8×8×0.625
7	W14×145	19	W14×426	7	W18×40	19	W24×84	7	HSS4×4×0.375	19	HSS9×9×0.625
8	W14×159	20	W14×455	8	W16×50	20	W27×94	8	HSS4-1/2×4–1/2×0.375	20	HSS10×10×0.625
9	W14×176	21	W14×500	9	W18×46	21	W27×102	9	HSS4×4×0.500	21	HSS10×10×0.750
10	W14×193	22	W14×550	10	W16×57	22	W27×114	10	HSS5×5×0.375	22	HSS12×12×0.750
11	W14×211	23	W14×605	11	W18×50	23	W30×108	11	HSS4-1/2×4–1/2×0.500	23	HSS14×14×0.875
12	W14×233	24	W14×665	12	W21×44	24	W30×116	12	HSS6×6×0.375		

Table 2 Optimal designs for 5-story CBF

Variables	Middle span (MS)			Side spans (SS)		
	IFWA	CMO	ECBO	IFWA	CMO	ECBO
C1	W14×48	W14×48	W14×48	W14×82	W14×53	W14×82
C2	W14×48	W14×48	W14×48	W14×48	W14×48	W14×68
C3	W14×48	W14×48	W14×48	W14×48	W14×48	W14×68
C4	W14×132	W14×132	W14×132	W14×82	W14×68	W14×82
C5	W14×53	W14×48	W14×48	W14×48	W14×48	W14×53
C6	W14×48	W14×48	W14×48	W14×48	W14×48	W14×53
Bm1	W12×35	W12×35	W12×35	W12×35	W12×35	W12×35
Br1	HSS8×8×0.500	HSS8×8×0.500	HSS10×10×0.625	HSS6×6×0.375	HSS6×6×0.375	HSS6×6×0.375
Br2	HSS6×6×0.500	HSS6×6×0.500	HSS6×6×0.500	HSS6×6×0.375	HSS6×6×0.375	HSS6×6×0.375
Br3	HSS6×6×0.500	HSS6×6×0.500	HSS6×6×0.500	HSS5×5×0.375	HSS5×5×0.375	HSS5×5×0.375
Br4	HSS6×6×0.375	HSS6×6×0.375	HSS6×6×0.375	HSS5×5×0.375	HSS5×5×0.375	HSS5×5×0.375
Br5	HSS6×6×0.375	HSS5×5×0.375	HSS5×5×0.375	HSS4×4×0.375	HSS4×4×0.375	HSS4×4×0.375
Best (kg)	12,635.8	12,459.2	12,897.7	13,222.7	12,469.1	13,900.9
Average (kg)	14,035.9	13,933.4	14,471.9	14,084.5	14,140.1	14,671.5
SD (kg)	1032.5	1091.0	1281.2	732.9	768.6	582.6
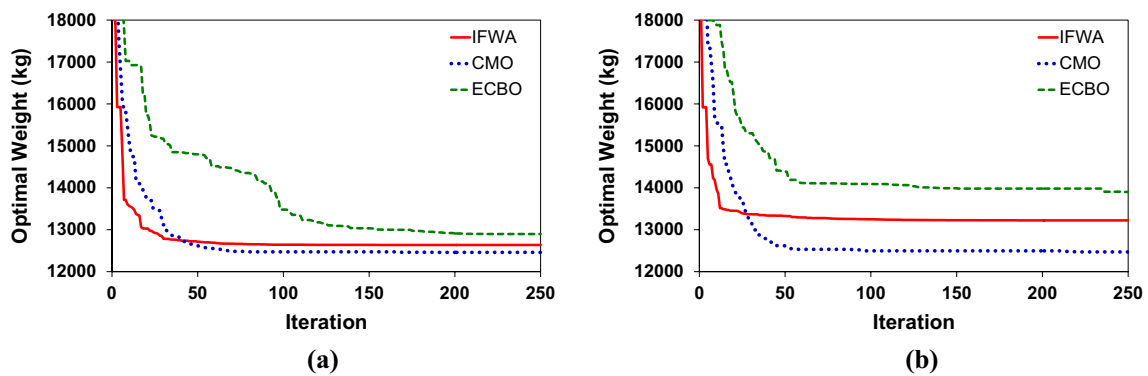
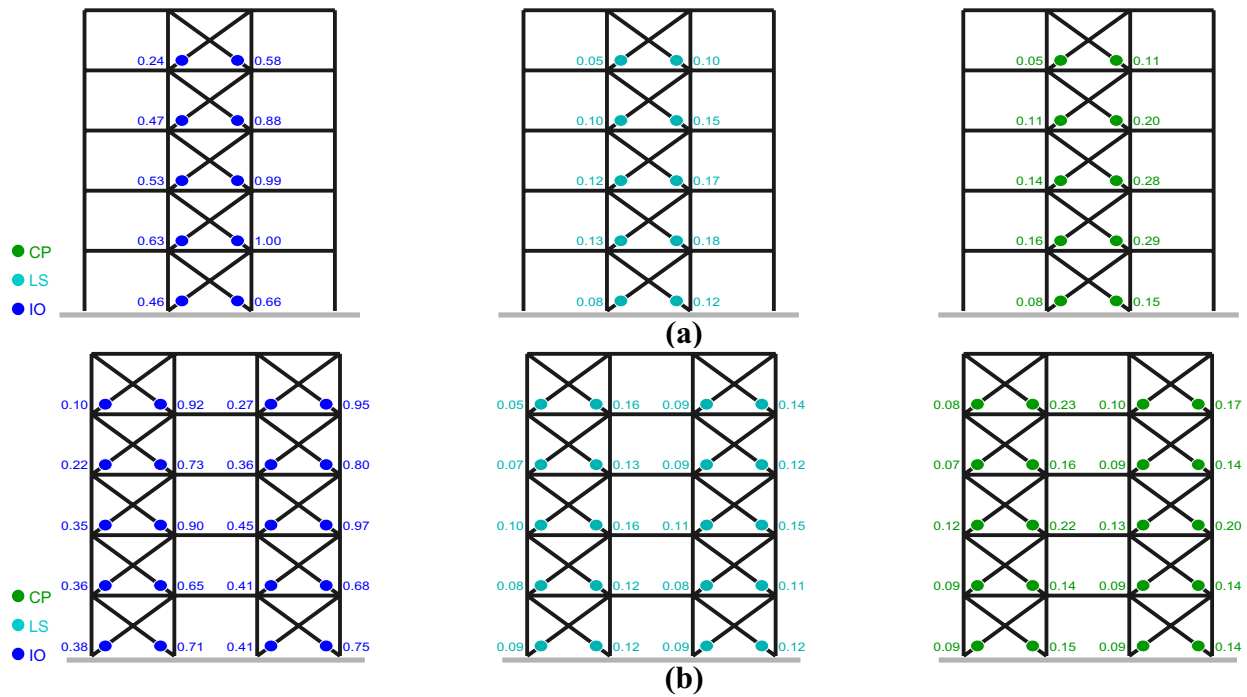**Fig. 2** Convergence histories of IFWA, CMO, and ECBO for **a** MS and **b** SS 5-story CBFs

Fig. 3 $\Delta/\Delta_{\mathrm{all}}$ of braces for optimum designs found by IFWA for **a** MS and **b** SS 5-story CBFs
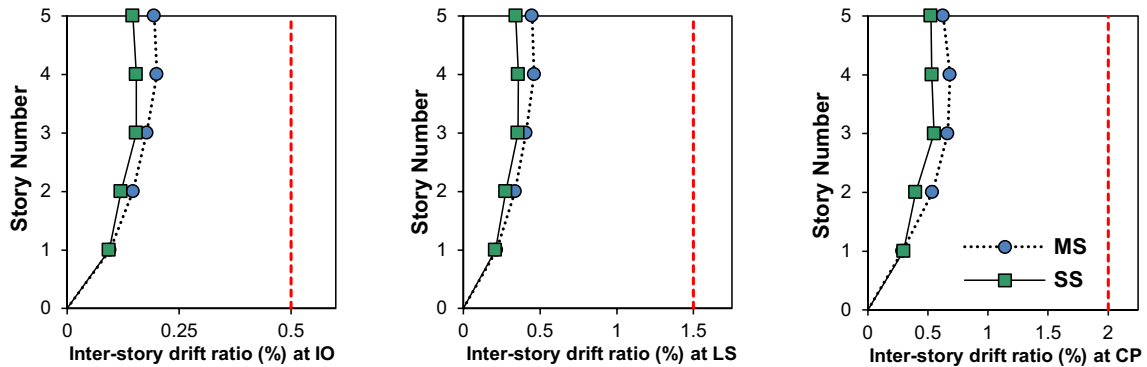

Fig. 4 Inter-story drift profile of optimum designs found by IFWA for **a** MS and **b** SS 5-story CBFs
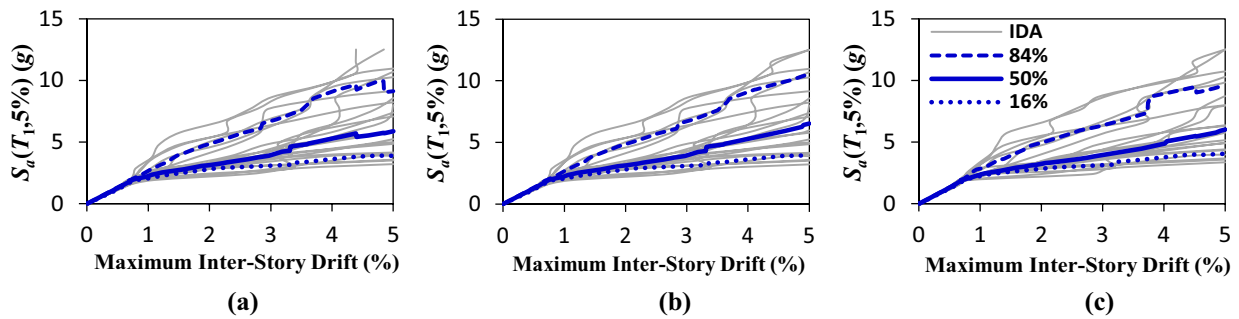

Fig. 5 IDA curves for MS model of optimal 5-story CBFs found by **a** IFWA, **b** CMO and **c** ECBO

respectively. The details of seismic assessment results are also presented in Table 3.

The results of the seismic assessment for 5-story CBFs demonstrate that the ACMR values for all optimal 5-story CBFs are much higher than permissible ACMR, which proves that optimal designs have considerable collapse safety. Furthermore, the solutions found by the CMO algorithm have the least structural weight and also have remarkable collapse capacity. It is worth-mentioning that the optimal SS 5-story CBF found by the ECBO algorithm has the highest ACMR, but it is not chosen as the best solution because it has the highest structural weight.

5.2 10-story CBF

The optimal designs of 10-story CBF found by IFWA, CMO, and ECBO algorithms are given in Table 4. In this example, 50 particles at 250 iterations are considered for

all the algorithms during the optimization process. Figure 8 depicts the convergence curves of these metaheuristic algorithms during the optimization process.

The results demonstrate the superiority of CMO over the IFWA and ECBO in terms of best weight, average weight and convergence rate in both the MS and SS optimization cases.

For the optimal design found by CMO, Fig. 9 shows the values of Δ/Δ_{all} for braces at different performance levels indicating that for both the optimal MS and SS models the axial deformation constraint of braces at IO level is the active constraint. Moreover, Fig. 10 shows the inter-story drifts along with the height of the structures. It can be seen that the inter-story drift constraints at all performance levels are not active. However, for the MS model the maximum inter-story drift at IO level is close to the limit value. The other constraints are not active in this optimization problem.
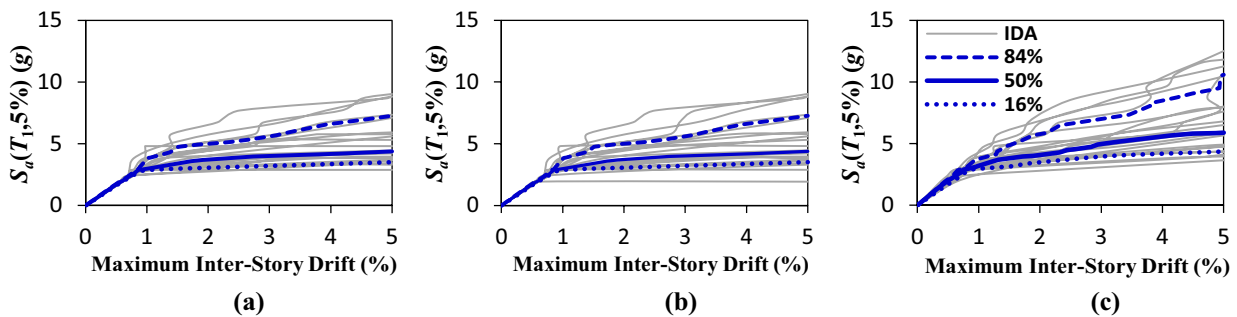

Fig. 6 IDA curves for SS model of optimal 5-story CBFs found by **a** IFWA, **b** CMO and **c** ECBO

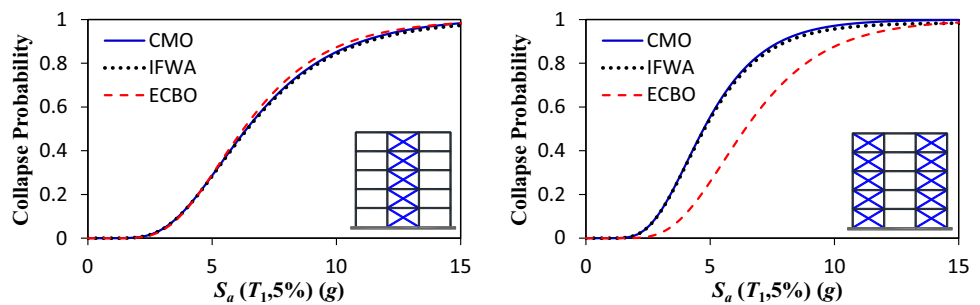**Fig. 7** Collapse fragility curves for MS and SS models of optimal 5-story CBFs

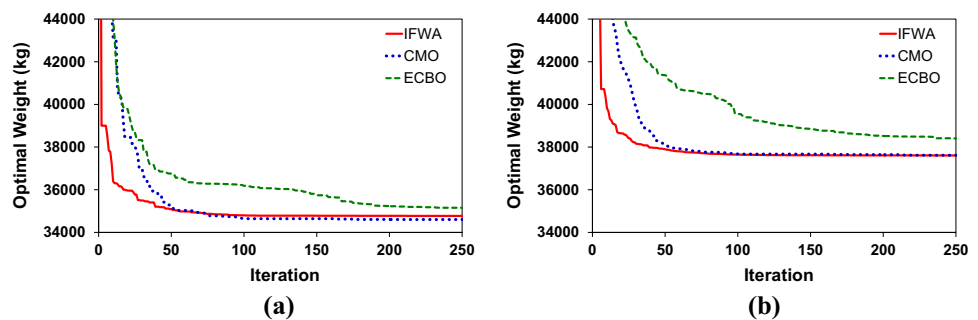**Table 3** Details of seismic assessment of optimal 5-story CBFs

Optimal designs		Weight (kg)	IM_{MCE} (g)	$IM_{50\%}$ (g)	CMR	SSF	ACMR	Acceptable ACMR [14]	Pass/fail
MS	IFWA	12,635.8	1.44	6.38	4.43	1.13	5.01	1.52	Pass
	CMO	12,459.2	1.44	6.35	4.41	1.13	4.98	1.52	Pass
	ECBO	12,897.7	1.44	6.22	4.32	1.13	4.88	1.52	Pass
SS	IFWA	13,222.7	1.44	4.74	3.29	1.15	3.78	1.52	Pass
	CMO	12,469.1	1.44	4.72	3.28	1.15	3.77	1.52	Pass
	ECBO	13,900.9	1.44	6.35	4.41	1.15	5.07	1.52	Pass

Table 4 Optimal designs for 10-story CBF

Variables	Middle span (MS)			Side spans (SS)		
	IFWA	CMO	ECBO	IFWA	CMO	ECBO
C1	W14×48	W14×48	W14×48	W14×193	W14×193	W14×193
C2	W14×48	W14×48	W14×48	W14×132	W14×145	W14×145
C3	W14×48	W14×48	W14×48	W14×82	W14×82	W14×132
C4	W14×48	W14×48	W14×48	W14×48	W14×48	W14×48
C5	W14×48	W14×48	W14×48	W14×48	W14×48	W14×48
C6	W14×311	W14×311	W14×311	W14×211	W14×193	W14×193
C7	W14×257	W14×257	W14×233	W14×145	W14×145	W14×145
C8	W14×145	W14×132	W14×145	W14×132	W14×82	W14×132
C9	W14×68	W14×68	W14×68	W14×48	W14×48	W14×48
C10	W14×48	W14×48	W14×48	W14×48	W14×48	W14×48
Bm1	W12×35	W12×35	W12×35	W12×35	W12×35	W12×35
Br1	HSS8×8×0.625	HSS8×8×0.625	HSS8×8×0.625	HSS6×6×0.625	HSS6×6×0.625	HSS6×6×0.625
Br2	HSS8×8×0.625	HSS8×8×0.625	HSS8×8×0.625	HSS6×6×0.500	HSS6×6×0.625	HSS6×6×0.500
Br3	HSS8×8×0.500	HSS8×8×0.500	HSS8×8×0.500	HSS6×6×0.500	HSS6×6×0.500	HSS6×6×0.500
Br4	HSS8×8×0.625	HSS8×8×0.625	HSS10×10×0.625	HSS6×6×0.500	HSS6×6×0.500	HSS6×6×0.500
Br5	HSS8×8×0.500	HSS8×8×0.625	HSS8×8×0.500	HSS6×6×0.500	HSS6×6×0.625	HSS6×6×0.500
Br6	HSS8×8×0.500	HSS8×8×0.500	HSS7×7×0.625	HSS6×6×0.500	HSS7×7×0.625	HSS6×6×0.375
Br7	HSS8×8×0.500	HSS8×8×0.500	HSS8×8×0.500	HSS6×6×0.375	HSS6×6×0.375	HSS6×6×0.375
Br8	HSS8×8×0.500	HSS8×8×0.500	HSS10×10×0.625	HSS6×6×0.375	HSS6×6×0.375	HSS6×6×0.375
Br9	HSS6×6×0.500	HSS6×6×0.500	HSS6×6×0.500	HSS6×6×0.375	HSS5×5×0.375	HSS5×5×0.375
Br10	HSS5×5×0.375	HSS5×5×0.375	HSS6×6×0.375	HSS4×4×0.375	HSS5×5×0.375	HSS5×5×0.375
Best (kg)	34,772.4	34,603.7	35,154.7	37,617.0	37,607.7	38,406.9
Average (kg)	40,025.6	38,562.2	39,513.6	39,852.0	39,438.0	39,683.4
SD (kg)	4038.5	3389.2	3418.6	1128.1	1061.5	834.4

Fig. 8 Convergence histories of IFWA, CMO, and ECBO for **a** MS and **b** SS 10-story CBFs


For the optimal designs of 10-story CBF found by IFWA, CMO, and ECBO algorithms, the IDA and collapse fragility curves are shown in Figs. 11, 12 and 13, respectively. Moreover, Table 5 summarizes the details of seismic assessment results.

It can be observed from Table 5 that for the optimal 10-story CBFs the computed *ACMR* values are higher than the acceptable one specified by FEMA-P695. This means that these optimally designed structures are of acceptable seismic collapse safety. In addition, the results demonstrate that the *ACMR* values of SS models of the optimal 10-story CBFs are higher than those of the MS models.

6 Conclusions

The present paper is devoted to assess the seismic collapse capacity of optimally designed steel concentrically braced frames in the context of performance-based design. To
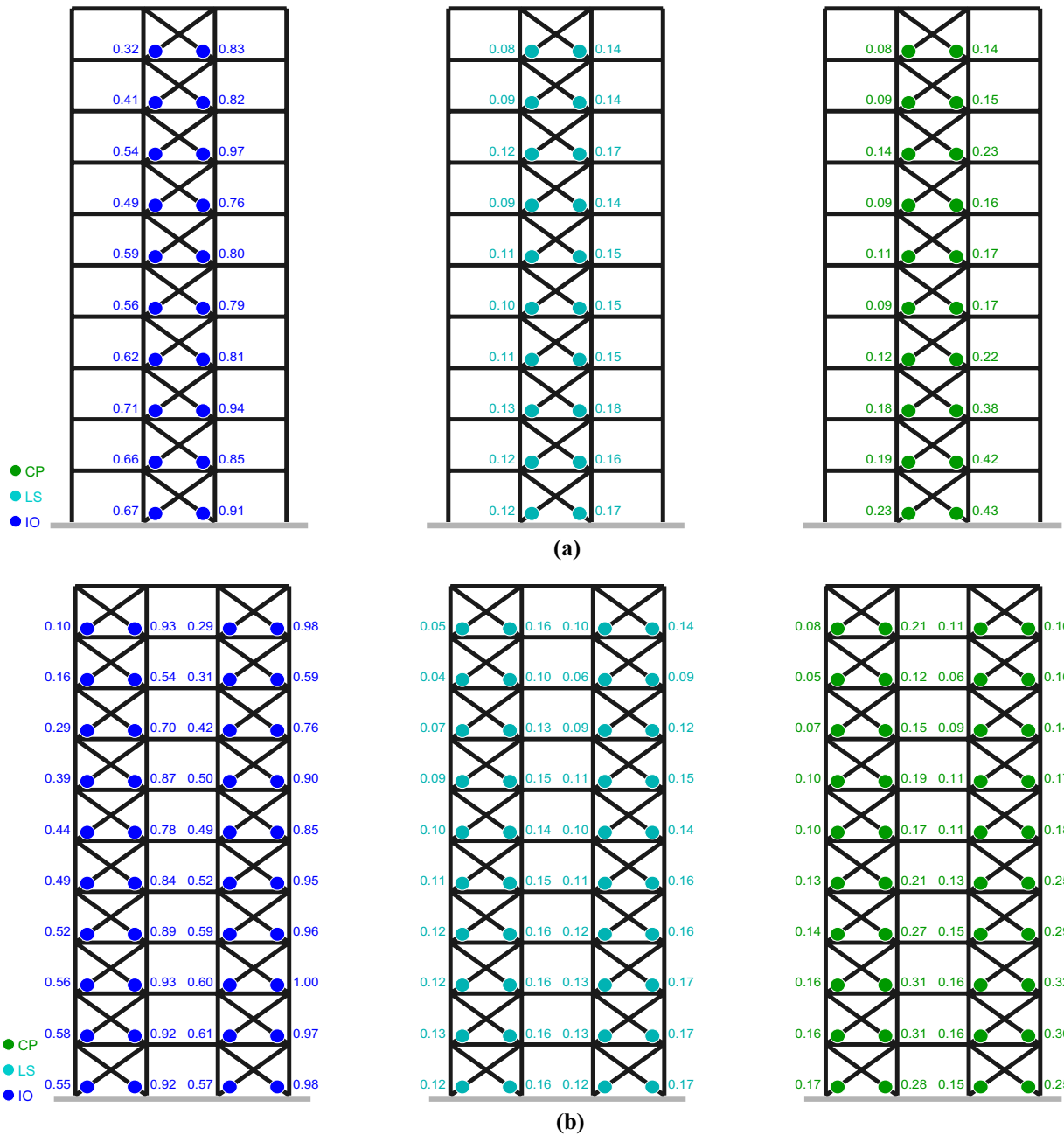
Fig. 9 Δ/Δ_{all} of braces for optimum designs found by IFWA for **a** MS and **b** SS 10-story CBFs

perform the optimization task three efficient metaheuristic algorithms, namely improved fireworks algorithm (IFWA), center of mass optimization (CMO), and enhanced colliding-bodies optimization (ECBO), are utilized. Incremental dynamic analysis (IDA) is performed to generate the seismic collapse fragility curves to compute the adjusted collapse margin ratio (ACMR) of optimally designed concentrically braced frames. Two illustrative examples of three-bays, 5- and 10-story frames with two different topologies of bracing systems, namely in the middle span

(MS), and the side spans (SS), are presented and the main findings of the present work are summarized as follows:

- CMO outperforms IFWA and ECBO in terms of optimal weight and convergence rate in the both MS and SS models of the 5- and 10-story frames.
- Axial deformation constraints of braces at IO performance level are active constraints in all the presented numerical examples.
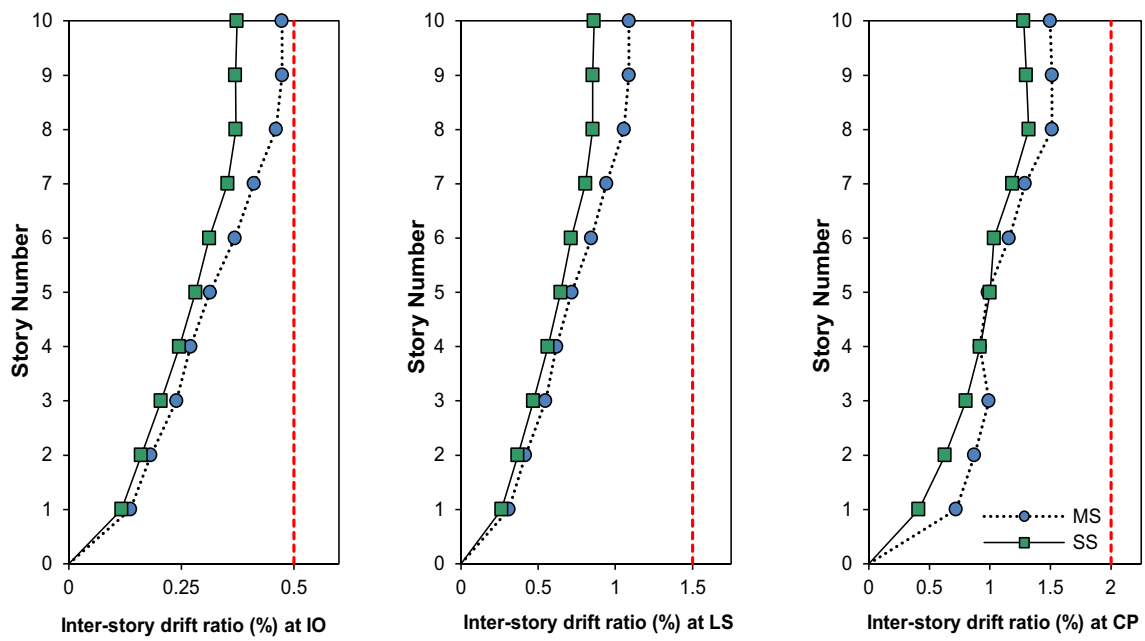
Fig. 10 Inter-story drift profile of optimum designs found by IFWA for **a** MS and **b** SS 10-story CBFs
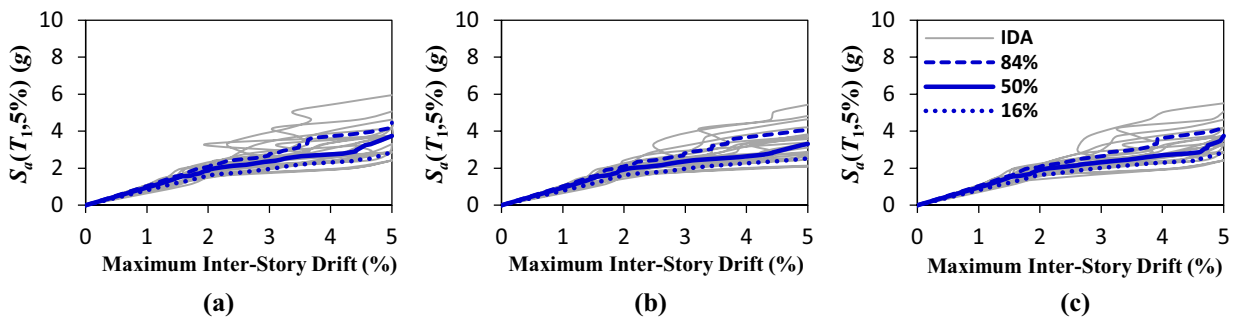

Fig. 11 IDA curves for MS model of optimal 10-story CBFs found by **a** IFWA, **b** CMO and **c** ECBO
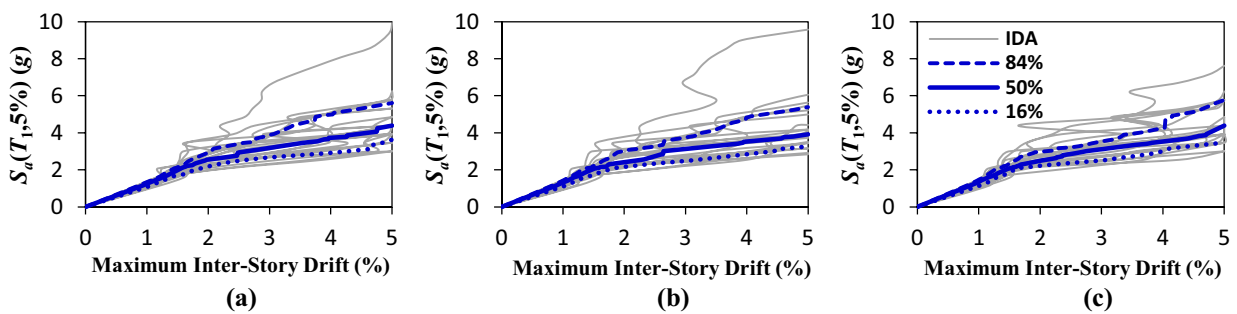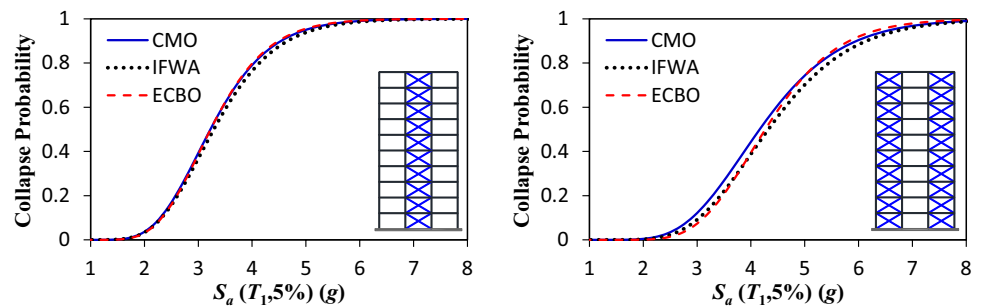

Fig. 12 IDA curves for SS model of optimal 10-story CBFs found by **a** IFWA, **b** CMO and **c** ECBO

Fig. 13 Collapse fragility curves for MS and SS models of optimal 10-story CBFs

Table 5 Details of seismic assessment of optimal 10-story CBFs

Optimal designs		Weight (kg)	IM_{MCE} (g)	$IM_{50\%}$ (g)	CMR	SSF	ACMR	Acceptable ACMR [14]	Pass/fail
MS	IFWA	34,772.4	1.65	3.29	1.99	1.13	2.25	1.52	Pass
	CMO	34,603.7	1.64	3.23	1.97	1.13	2.22	1.52	Pass
	ECBO	35,154.7	1.65	3.22	1.95	1.13	2.20	1.52	Pass
SS	IFWA	37,617.0	1.73	4.33	2.50	1.12	2.80	1.52	Pass
	CMO	37,607.7	1.73	4.16	2.40	1.12	2.69	1.52	Pass
	ECBO	38,406.9	1.73	4.26	2.46	1.12	2.76	1.52	Pass

- The MS and SS models of optimal 5- and 10-story braced frames found by all algorithms have acceptable seismic collapse capacity.
- Mean ACMR values of MS and SS models of optimally designed 5-story braced frame are, respectively, 4.96 and 4.21, which are significantly larger than the acceptable ACMR of 1.52.
- For the MS and SS models of optimally designed 10-story braced frame, mean ACMR values are, respectively, 2.22 and 2.75, which are larger than the acceptable ACMR of 1.52.
- For the optimal 5-story braced frames, the mean ACMR of MS model is higher than that of SS model. This means that the MS model is of higher seismic collapse capacity compared to the SS model. Conversely, in the case of 10-story braced frames the SS model has higher seismic collapse safety than the MS model.

References

1. ASCE-41-13 (2014) Seismic evaluation and retrofit of existing buildings. American Society of Civil Engineers, Reston
2. Fragiadakis M, Vamvatsikos D, Karlaftis MG, Lagaros ND, Papadrakakis M (2015) Seismic assessment of structures and lifelines. J Sound Vib 334:29–56
3. Gholizadeh S, Fattahi F (2019) Multi-objective design optimization of steel moment frames considering seismic collapse safety. Eng Comput (In press). https://doi.org/10.1007/s00366-019-00886-y
4. Hassanzadeh A, Gholizadeh S (2019) Collapse-performance-aided design optimization of steel concentrically braced frames. Eng Struct 197:109411
5. Degertekin SO, Tutar H, Lamberti L (2020) School-based optimization for performance-based optimum seismic design of steel frames. Eng Comput (In press). https://doi.org/10.1007/s00366-020-00993-1
6. Bertero VV (1977) Strength and deformation capacities of buildings under extreme environments. Struct Eng Struct Mech 53:29–79
7. Bazzurro P, Cornell CA (1994) Seismic hazard analysis of nonlinear structures. I: methodology. J Struct Eng 120:3320–3344
8. Vamvatsikos D, Cornell CA (2002) Incremental dynamic analysis. Earthq Eng Struct Dyn 31(3):491–514. https://doi.org/10.1002/eqe.141
9. Vamvatsikos D, Cornell CA (2004) Applied incremental dynamic analysis. Earthq Spectra 20:523–553
10. Brunesi E, Nascimbene R, Parisi F, Augenti N (2015) Progressive collapse fragility of reinforced concrete framed structures through incremental dynamic analysis. Eng Struct 104:65–79
11. Wijesundara KK, Bolognini D, Nascimbene R, Calvi GM (2009) Review of design parameters of concentrically braced frames with rhs shape braces. J Earthq Eng 13:109–131
12. Wijesundara KK, Nascimbene R, Rassati GA (2018) Evaluation of the seismic performance of suspended zipper column concentrically braced steel frames. J Constr Steel Res 150:452–461
13. Gholizadeh S, Milany A (2018) An improved fireworks algorithm for discrete sizing optimization of steel skeletal structures. Eng Optim 50:1829–1849
14. Gholizadeh S, Ebadijalal M (2018) Performance based discrete topology optimization of steel braced frames by a new metaheuristic. Adv Eng Softw 123:77–92
15. Kaveh A, Ilchi Ghazaan M (2014) Enhanced colliding bodies optimization for design problems with continuous and discrete variables. Adv Eng Softw 77:66–75
16. FEMA P-695 (2009) Quantification of building seismic performance factors. Federal Emergency Management Agency, Washington (DC)

17. OpenSees (2012) Version 2.4.0. PEER, Berkeley
18. MATLAB (2016) The Language of Technical Computing. The MathWorks Inc.
19. AISC-LRFD (2001) Manual of steel construction: load & resistance factor design, 2nd edn. American Institute of Steel Construction, Chicago
20. Vanderplaats G (1984) Numerical optimization techniques for engineering design: with application. McGraw-Hill, New York
21. Tan Y, Zhu Y (2010) Fireworks Algorithm for Optimization. Springer, Berlin
22. Tan Y (2015) Fireworks Algorithm, A Novel Swarm Intelligence Optimization Method. Peking University, Beijing
23. FEMA-274 (1997) NEHRP commentary on the guidelines for the seismic rehabilitation of buildings. Federal Emergency Management Agency, Washington, DC